APPLICATION OF CONTROL THEORY IN THE FORMATION OF A TIMESCALE

P. Koppang, D. Johns, and J. Skinner
U.S. Naval Observatory

Abstract

We have created a timescale that joins the short-term stability of several hydrogen masers with the long-term capabilities of an ensemble of cesium frequency standards. Control theory is utilized in a system design that combines frequency standards with varied properties. The system steers a maser ensemble with respect to a cesium ensemble while minimally perturbing the maser short-term performance. Results are given from both simulated and measured data. Systems are designed using linear quadratic Gaussian (LQG) and pole-placement techniques.

INTRODUCTION

One of the many challenges in the construction of a timescale (mean) is the combination of frequency standards with dissimilar stochastic properties. A common example for timing institutions, and one that is addressed in this paper, is that of combining hydrogen masers and cesium standards. The hydrogen masers are approximately an order of magnitude more stable than the cesium standards in the short term, while the cesium standards show better long-term characteristics. There are roughly 60 cesium standards and 15 hydrogen masers contributing to the U.S. Naval Observatory (USNO) operational timescale at any given time. These standards are spread throughout several locations at USNO in Washington, DC.

BASIC DESIGN

Figure 1 is a block diagram that shows the overall design of the system. It is comprised of two coupled subsystems. One subsystem is created by steering a maser mean (MM) to a steered cesium mean (CM) **[1]**. The cesium mean steers are those used to align it with UTC.

The other subsystem creates the physical output by steering the output of a maser to the MM with a precision frequency synthesizer referred to as an AOG.

The filter utilized in both subsystems is a Kalman filter **[2-4]**.

The present Master Clock (MC) control design steers a maser-based AOG signal once a day to a dynamically weighted timescale **[1]**. The prototype designs use hourly steers and the masers have had deterministic rates and drifts with respect to the cesium mean removed.

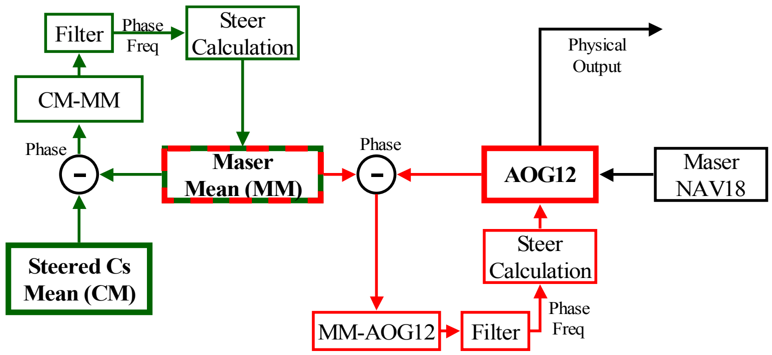

Figure 1. Design Block Diagram.

STATE-SPACE MODEL

The performance of frequency standards may be described using state-space modeling techniques **[3,4,5]**. The state-space model for the system described in Figure 1 is

$$\mathbf{X}_{t+\tau} = \mathbf{\Phi}\mathbf{X}_t + \mathbf{B}u_t$$

$$\mathbf{X} = \begin{bmatrix} x_{MM-AOG12} \\ y_{MM-AOG12} \\ x_{CM-MM} \\ y_{CM-MM} \end{bmatrix}, \ \mathbf{\Phi} = \begin{bmatrix} 1 & \tau & 0 & 0 \\ 0 & 1 & 0 & 0 \\ 0 & 0 & 1 & \tau \\ 0 & 0 & 0 & 1 \end{bmatrix}, \text{ and } \mathbf{B} = \begin{bmatrix} \tau & -\tau \\ 1 & -1 \\ 0 & \tau \\ 0 & 1 \end{bmatrix}$$

x is phase difference, *y* is frequency difference, and the control $u_t = -\mathbf{G}\mathbf{X}_t$, where $\mathbf{G}$ is the control gain. The above equation can now be rewritten as $\mathbf{X}_{t+\tau} = (\mathbf{\Phi} - \mathbf{B}\mathbf{G})\mathbf{X}_t$.

PROTOTYPE SYSTEM DESIGN

The linear quadratic Gaussian (LQG) design technique was utilized for the first implementation of this system. In LQG theory **[1,3,5-7]**, the system is modeled with a linear state-space equation with Gaussian noise characteristics. The optimal control minimizes a quadratic cost function:

$$J = \sum_t [\mathbf{X}_t^T \mathbf{W}_Q \mathbf{X}_t + \mathbf{u}_t^T \mathbf{W}_R \mathbf{u}_t]$$

where,

$$\mathbf{X}_t = \begin{bmatrix} x \\ y \end{bmatrix}_t = \begin{bmatrix} \text{phase offset} \\ \text{frequency offset} \end{bmatrix}, \text{ and}$$

$\mathbf{u}$ is a vector representing the control $\mathbf{u}_t = -\mathbf{G}\mathbf{X}_t$.

The cost matrix weighting for state offsets is $\mathbf{W}_Q$ and the cost for the control effort $\mathbf{W}_R$. The solution to minimizing the quadratic cost function **J** can be shown to yield **[1,3,5-7]**:

$$\hat{\mathbf{G}} = (\mathbf{B}^T\hat{\mathbf{K}}\mathbf{B} + \mathbf{W}_R)^{-1}\mathbf{B}^T\hat{\mathbf{K}}\mathbf{\Phi},$$

where $\hat{K}$ is a solution to the steady-state Riccati equation

$$\hat{\mathbf{K}} = \mathbf{\Phi}^T\hat{\mathbf{K}}\mathbf{\Phi} + \mathbf{W}_Q - \mathbf{\Phi}^T\hat{\mathbf{K}}\mathbf{B}(\mathbf{B}^T\hat{\mathbf{K}}\mathbf{B} + \mathbf{W}_R)^{-1}\mathbf{B}^T\hat{\mathbf{K}}\mathbf{\Phi}.$$

Weighting matrices were tested using simulations until a control system was obtained that provided minimal short-term steering perturbations along with small time and frequency offsets. The weighting matrices selected based on the simulations were

$$\mathbf{W}_Q = \begin{bmatrix} 2.5\text{e-}15 & 0 & 0 & 0 \\ 0 & 1.7\text{e-}7 & 0 & 0 \\ 0 & 0 & 2.5\text{e-}17 & 0 \\ 0 & 0 & 0 & 2.8\text{e-}8 \end{bmatrix}, \text{ and } \mathbf{W}_R = \begin{bmatrix} 2.5\text{e-}3 & 0 \\ 0 & 1 \end{bmatrix}.$$

The control gain calculated from the Riccati equation is

$$\mathbf{G} = \begin{bmatrix} -7.4\text{e-}8 & -0.024 & -4.37\text{e-}9 & -0.0056 \\ 1.79\text{e-}10 & 4.65\text{e-}5 & -4.98\text{e-}9 & -0.006 \end{bmatrix}.$$

Figures 2 and 3 show the performance of the initial design as measured during actual real-time operational system testing. The time and frequency offsets were acceptable, but the frequency stability of the system for averaging times greater than 30,000 seconds was not making an improvement over the present operational master clock steering design.

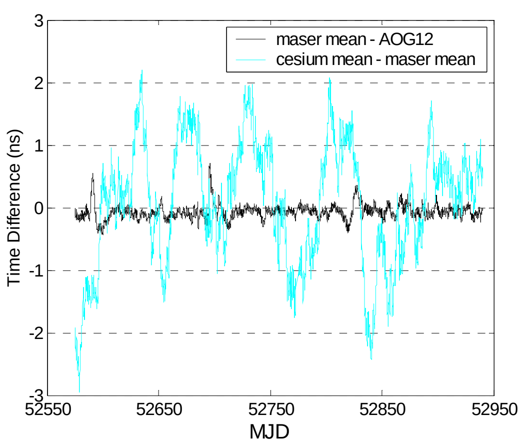

Figure 2. Measured Time Difference Data.

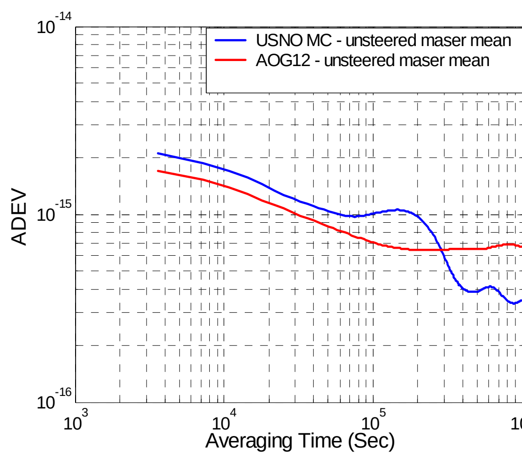

Figure 3. Stability Comparison.

SYSTEM REDESIGN

Although the system performed well, it was decided to redesign the control in an attempt to improve the longer-term frequency stability of the physical output. The redesign was done using pole-placement techniques in order to attempt to get a better handle on the system time constants. The two-state model for a frequency standard steered utilizing discrete frequency steps is given by

$$\mathbf{X}_{t+\tau} = \mathbf{\Phi X}_t + \mathbf{B}u_t \ ,$$

where $\mathbf{X} = \begin{bmatrix} x \\ y \end{bmatrix} = \begin{bmatrix} \text{phase offset} \\ \text{frequency offset} \end{bmatrix}$, $\mathbf{\Phi} = \begin{bmatrix} 1 & \tau \\ 0 & 1 \end{bmatrix}$, $u_t = -\mathbf{GX}_t = -\begin{bmatrix} g_x & g_y \end{bmatrix}\begin{bmatrix} x \\ y \end{bmatrix}$, and $\mathbf{B} = \begin{bmatrix} \tau \\ 1 \end{bmatrix}$.

Given the gain $\mathbf{G}$, the state-space equation can be written as

$$\begin{bmatrix} x \\ y \end{bmatrix}_{t+\tau} = \begin{bmatrix} 1-g_x\tau & (1-g_y)\tau \\ -g_x & 1-g_y \end{bmatrix}\begin{bmatrix} x \\ y \end{bmatrix}_t = \mathbf{A}\begin{bmatrix} x \\ y \end{bmatrix}_t .$$

The eigenvalues of **A** correspond to the system poles and are related to the response of the system. The relationship between the control gain and the system poles can be solved from

$$\left| z\,\mathrm{I} - \begin{bmatrix} 1-g_x\tau & (1-g_y)\tau \\ -g_x & 1-g_y \end{bmatrix} \right| = z^2 + (g_y + \tau g_x - 2)z + 1 - g_y = 0 ,$$

where z relates to the z-transform and **I** is the identity matrix **[7]**. By equating terms in the above equation with the eigenvalue equation, one can solve for the control gains.

If we assume each subsystem is critically damped, then

$$g_x = \tau^{-1}\left(1 - \exp\left[-\tau/\mathrm{T_c}\right]\right)^2$$
$$g_y = 1 - \exp\left[-2\tau/\mathrm{T_c}\right],$$

where τ is the constant interval between steers and $\mathrm{T_c}$ is the approximate time constant.

We based the control gain time constants for the coupled system on the assumption that it was actually separated into two independent two-state systems. The time constant chosen for the maser mean to cesium mean subsystem was 30 days and the time constant for steering the AOG to the maser mean was 4 days. The control gain was calculated to be

$$\mathbf{G} = \begin{bmatrix} -3.0\text{e}-8 & -0.02 & 0 & 0 \\ 0 & 0 & -5.35\text{e}-10 & -0.0027 \end{bmatrix}.$$

Figures 4-6 show the response of the two system designs to initial 5×10^{-15} frequency offsets of the cesium mean, maser mean, and the AOG.

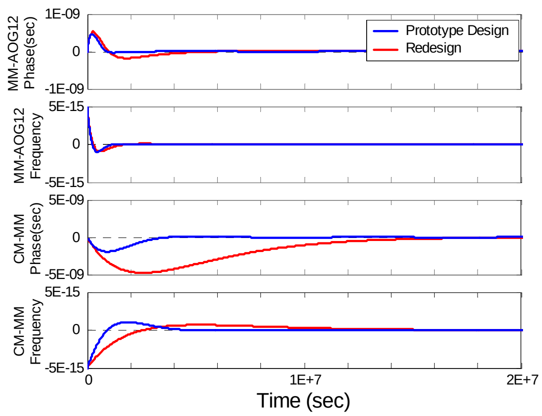

Figure 4. Responses to MM frequency offset.

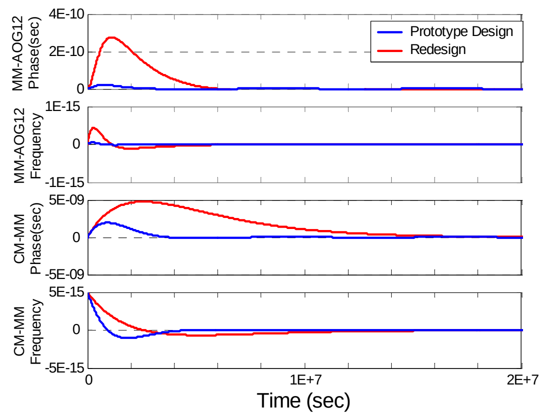

Figure 5. Responses to CM frequency offset.

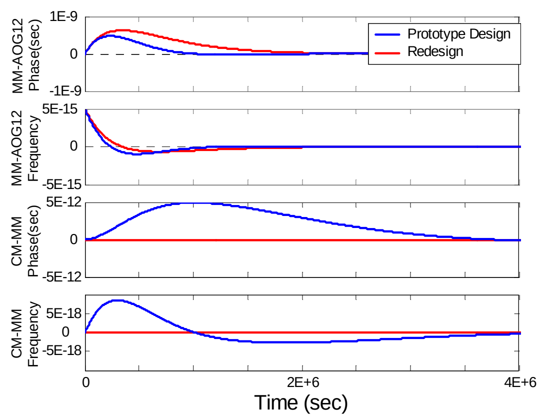

Figure 6. Responses to AOG frequency offset.

A comparison of the measured performance of the initial design and the simulated performance of the system redesign is shown in Figure 7. The redesign shows improved mid to long-term stability performance. Figure 8 shows the stability of the underlying maser and illustrates a decrease in the control effort of the simulated redesign compared to the actual steers implemented with AOG12.

CONCLUSION

Two control theory design techniques were utilized in a scheme for combining frequency standards that exhibit different frequency stability properties to make a physically realizable output of a timescale. The techniques are both appropriate for designing this system. The first prototype design gave a 35% improvement as measured by the Allan deviation at 2 days compared to the present Master Clock. The redesign promises to also improve the mid-term performance without the long-term degradation seen by the prototype design. We plan to continue investigating the problem and hope to gain more insight into improving our understanding of how system response characteristics influence the overall performance. This will likely include tests on how controlling each maser individually affects the system.

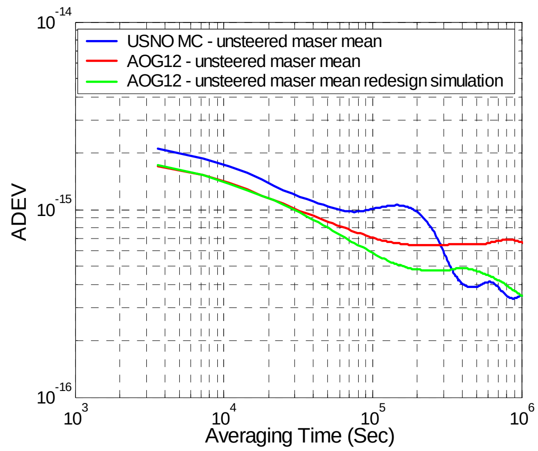

Figure 7. Stability comparison of different designs.

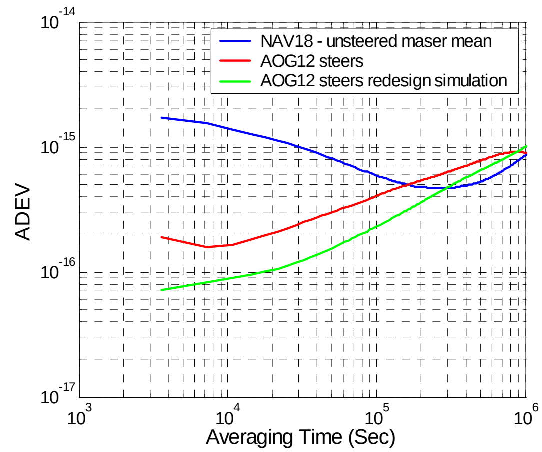

Figure 8. Control effort comparison.

REFERENCES

[1] D. Matsakis, M. Miranian, and P. Koppang, 1999, *"Steering the U.S. Naval Observatory (USNO) Master Clock,"* in Proceedings of the 1999 ION National Technical Meeting, 25-27 January 1999, San Diego, California, USA (Institute of Navigation, Alexandria, Virginia), pp. 871-879.

[2] R. Brown and P. Hwang, 1992, **Introduction to Random Signals and Applied Kalman Filtering,** second edition (John Wiley & Sons, New York).

[3] P. Koppang and R. Leland, 1999, *"Linear quadratic stochastic control of atomic hydrogen masers,"* **IEEE Transactions on Ultrasonics, Ferroelectrics, and Frequency Control, UFFC-46,** 517-522.

[4] J. Skinner and P. Koppang, 2002, *"Effects of parameter estimation and control limits on steered frequency standards,"* in Proceedings of the 33rd Annual Precise Time and Time Interval (PTTI) Systems and Applications Meeting, 27-29 November 2001, Long Beach, California, USA (U.S. Naval Observatory, Washington, D.C.), pp. 399-405.

[5] P. Koppang and P. Wheeler, 1998, *"Working application of TWSTT for high precision remote synchronization,"* in Proceedings of the 1998 IEEE International Frequency Control Symposium, 27-29 May 1998, Pasadena, California, USA (IEEE Publication 98CH36165), pp. 273-277.

[6] P. Koppang and D. Matsakis, 2000, *"New steering strategies for the USNO Master Clock,"* in Proceedings of the 31st Precise Time and Time Interval (PTTI) Systems and Applications Meeting, 7-9 December 1999, Dana Point, California, USA (U.S. Naval Observatory, Washington, D.C.), pp. 277-283.

[7] K. Ogata, 1995, **Discrete-Time Control Systems,** second edition (Prentice Hall, Englewood Cliffs, New Jersey).